Electronic Supplementary Information (ESI) for

Rapid preparation of water-soluble Ag@Au nanoclusters with bright deep-red emission

Miao-Miao Yin [a,b] , Wen-Qi Chen [a], Yan-Jun Hu [b], Yi Liu [a,c] and Feng-Lei Jiang *[,a]

[a] Sauvage Center for Molecular Sciences, College of Chemistry and Molecular Sciences, Wuhan University, Wuhan 430072, P. R. China

[b] Hubei Key Laboratory of Pollutant Analysis & Reuse Technology, College of Chemistry and Chemical Engineering, Hubei Normal University, Huangshi 435002, P. R. China

[c] College of Chemistry and Chemical Engineering, Tiangong University, Tianjin 300387, P. R. China

*Author to whom correspondence should be addressed. Email: fljiang@whu.edu.cn. Telephone: +86-27-68756667

Experimental section

Materials, Instruments and Methods

Materials. The reduced L-glutathione (GSH), hydrogen tetrachloroaurate trihydrate ($HAuCl_4 \cdot 3H_2O$) and silver nitrate (AgCl) were purchased from Sigma-Aldrich. Other chemicals were purchased from Sinopharm Chemical Reagent Co. (China). Ultrapure water (18.2 MΩ cm^{-1}, Millipore) was used to prepare all aqueous solutions.

Instruments. A Cary 100 fluorophotometer (Agilent, United States) was used to perform the fluorescence properties of NCs. The excitation wavelength was set as 400 nm and the fluorescence emission range was set as 500 to 850 nm. All tests were performed three times and then averaged. Fluorescence QYs and lifetimes were measured using FLS1000 (Edinburgh, United Kingdom). A Cary 100 UV-vis spectrophotometer (Agilent, USA) was used to record the UV-vis absorption spectra. TEM images were recorded on a JEOL JEM-2100 (HR) electron microscope. X-ray photoelectron spectroscopy and Auger electron spectroscopy were used to analyze the elemental composition of NCs (Thermo Fisher, ESCALAB 250Xi). Native polyacrylamide gel electrophoresis (PAGE) was carried out on a Bio-Rad Mini-PROTEAN Tetra system. Stacking and resolving gels were prepared from 4 and 30 wt % acrylamide monomers, respectively. The electrophoresis was allowed to run for ~4 h at a constant voltage of 150 V at 4 °C. The PB-10 standard pH meter (Sartorius, Germany) was used to measure the pH of solutions.

Methods.

Syntheses of O-AuNCs and R-AuNCs. All glassware was used after being soaked in aqua regia overnight and rinsed with double distilled water. Aqueous solutions of $HAuCl_4$ (1%, 1 mL) and GSH (100 mM, 0.364 mL) were mixed with 20 mL of ultrapure water at 25 °C. The reaction mixture was divided into two copies, one of which was heated to boiling after the turbidity disappeared under stirring for 1.5 h, and the other of which was added with 0.7 mL of 0.2 M NaOH solution and heated to boiling under stirring for 24 min. During the heating process, the color of the first reaction solution changed from colorless to light yellow and that of the second reaction solution changed from colorless to reddish brown. We named the products of the first reaction as O-

AuNCs and named the products of the second reaction as R-AuNCs.

Synthesis of O-Ag@AuNCs. Aqueous solutions of $HAuCl_4$ (1%, 0.5 mL) and GSH (100 mM, 0.182 mL) were mixed with 10 mL of ultrapure water at 25 °C. Subsequently, $AgNO_3$ (12 mM, 0.2 mL) was added to the mixture under gentle stirring (500 rpm). The reaction mixture was heated to boiling after the turbidity disappeared under stirring for 15 min. During the heating process, the color of the solution changed from colorless to light yellow, indicating the O-Ag@AuNCs were obtained. The as-prepared O-Ag@AuNCs were used after dialysis with a 3500 Da dialysis membrane for 24 h. The dialysis water was renewed every 4 h.

Synthesis of R-Ag@AuNCs. The synthetic method for the R-Ag@AuNCs has been modified slightly based on the above synthetic method for O-Ag@AuNCs. Aqueous solutions of $HAuCl_4$ (1%, 0.5 mL) and GSH (100 mM, 0.182 mL) were mixed with 10 mL of ultrapure water at 25 °C. Subsequently, $AgNO_3$ (12 mM, 0.2 mL) was added to the mixture under gentle stirring (500 rpm). Finally, NaOH (0.2 M, 0.7 mL) was added to the reaction solution and the turbidity disappeared immediately. The solution in the vessel was boiling under vigorous stirring for about 15 min. During the heating process, the color of the solution changed from colorless to reddish brown, indicating that the generated products were different from the above reaction. The as-prepared R-Ag@AuNCs were used after dialysis with a 3500 Da dialysis membrane for 24 h. The dialysis water was renewed every 4 h.

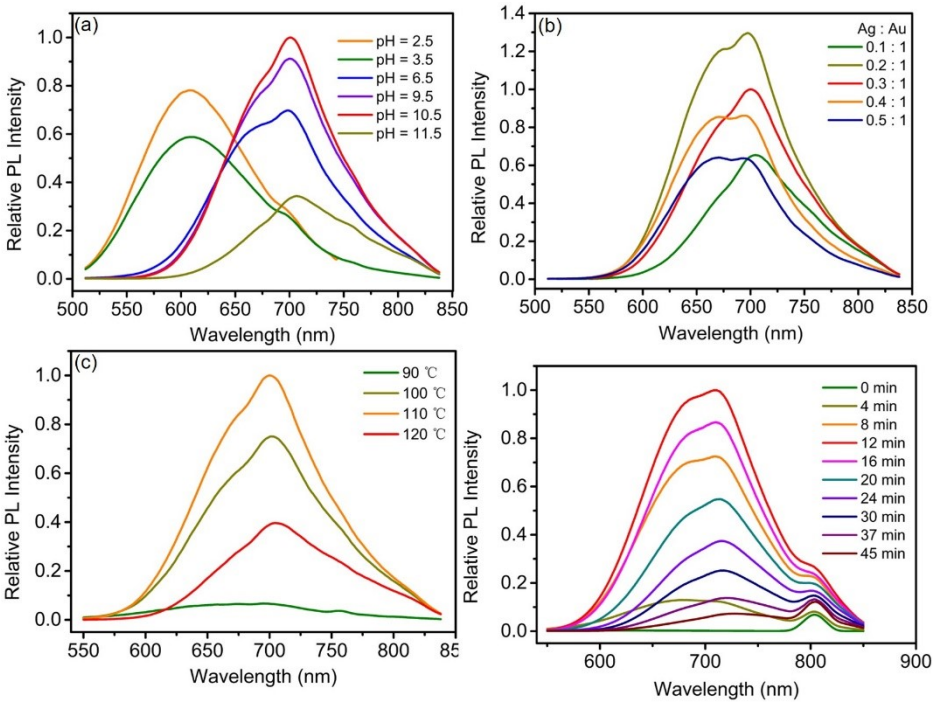

Fig. S1 The fluorescence emission spectra of R-Ag@AuNCs obtained at different pH (a), ratio of Ag : Au (b), temperature (c) and time (d).

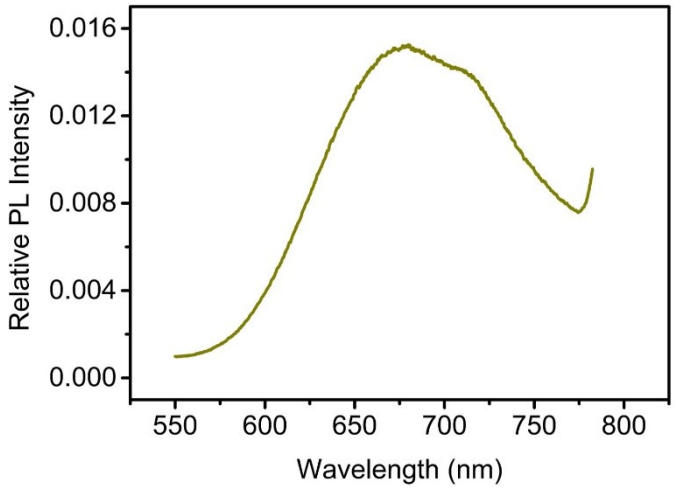

Fig. S2 Fluorescence emission spectra of R-AuNCs.

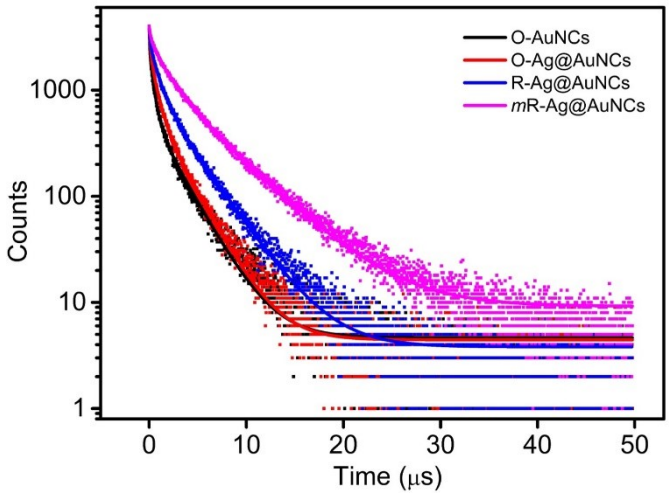

Fig. S3 Fluorescence decay of O-AuNCs, O-Ag@AuNCs, R-Ag@AuNCs and *m*R-Ag@AuNCs.

Table S1 Fluorescence lifetimes of O-AuNCs, O-Ag@AuNCs, R-Ag@AuNCs and *m*R-Ag@AuNCs.

	τ_1 (μs)	τ_2 (μs)	τ_3 (μs)	τ_{av} (μs)
O-AuNCs	0.445 (43.1%)	2.577 (14.9%)	0.057 (42.0%)	1.794
O-Ag@AuNCs	0.593 (44.6%)	0.094 (35.5%)	2.505 (19.9%)	1.768
R-Ag@AuNCs	3.252 (28.2%)	0.826 (42.9%)	0.098 (28.9%)	2.522
*m*R-Ag@AuNCs	1.404 (39.5%)	4.908 (39.2%)	0.151 (21.3%)	4.073

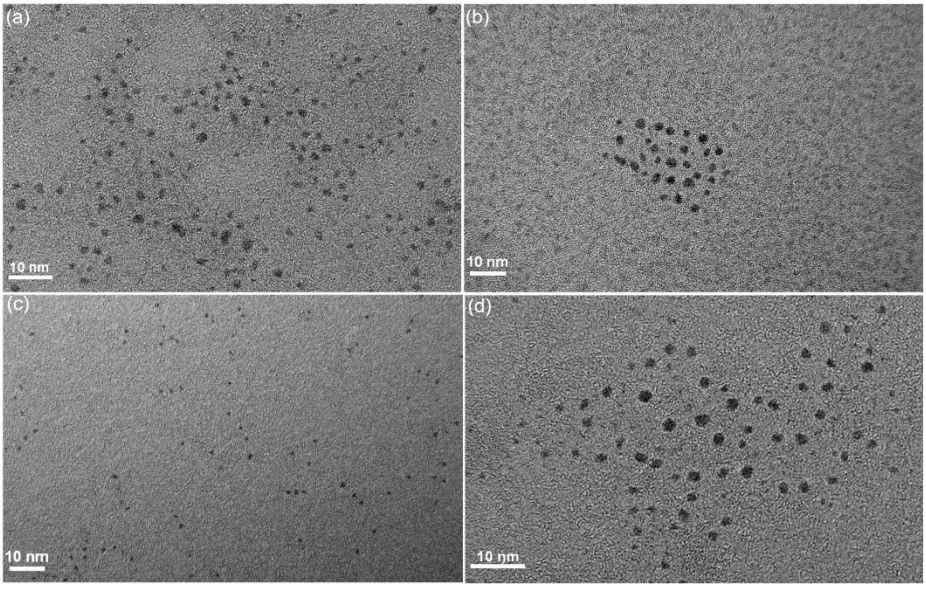

Fig. S4 TEM images of O-AuNCs (a), R-AuNCs (b), O-Ag@AuNCs (c) and R-Ag@AuNCs (d).

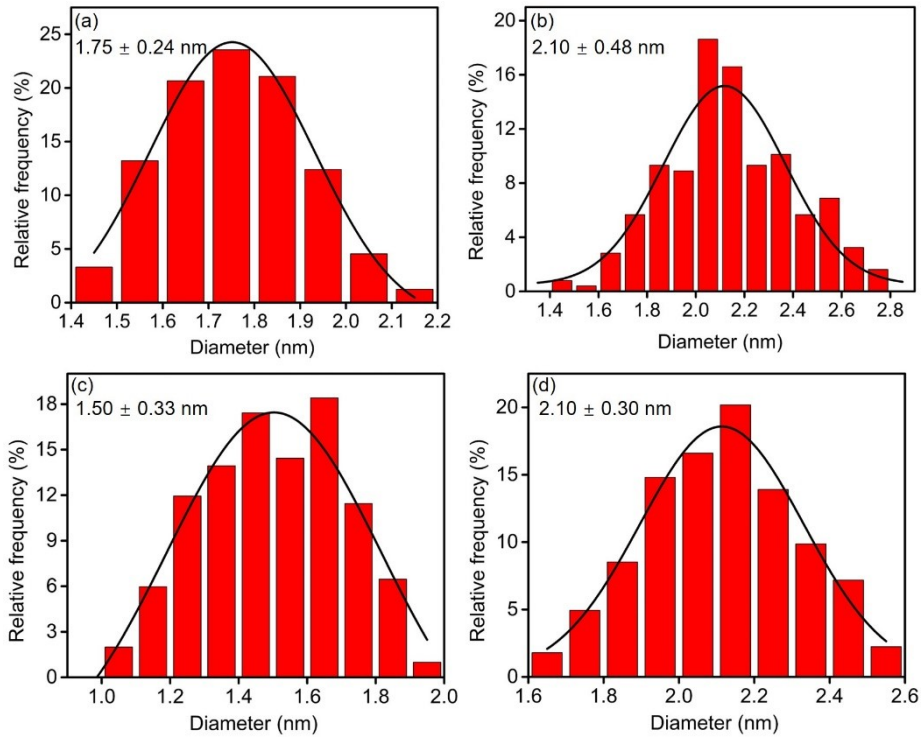

Fig. S5 Size distributions of O-AuNCs (a), R-AuNCs (b), O-Ag@AuNCs (c) and R-Ag@AuNCs (d). 200 particles were counted for statistical analysis.

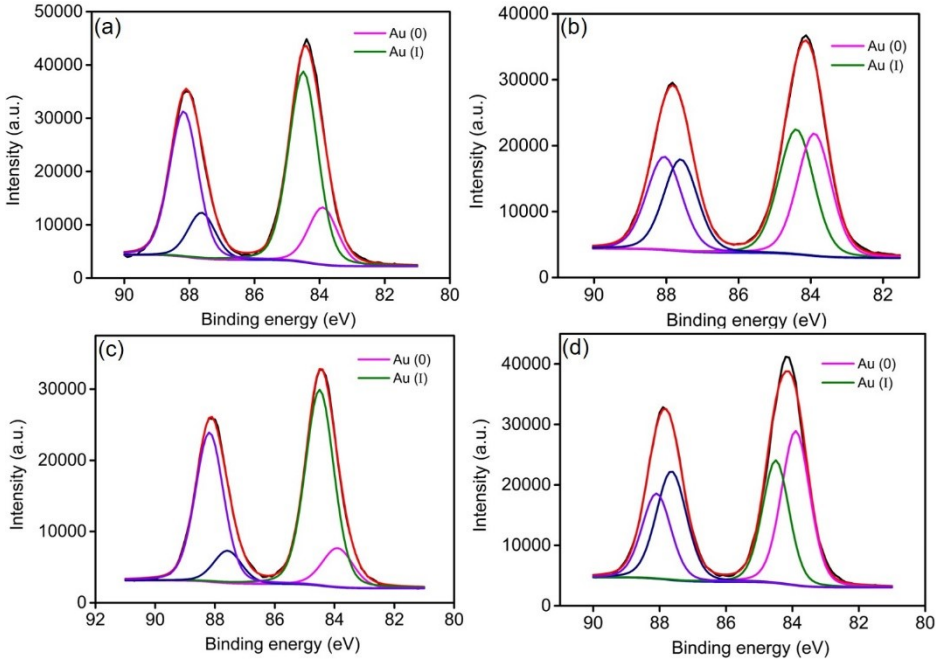

Fig. S6 XPS characterizations of Au 4f species of O-AuNCs (a), R-AuNCs (b), O-Ag@AuNCs (c) and R-Ag@AuNCs (d).

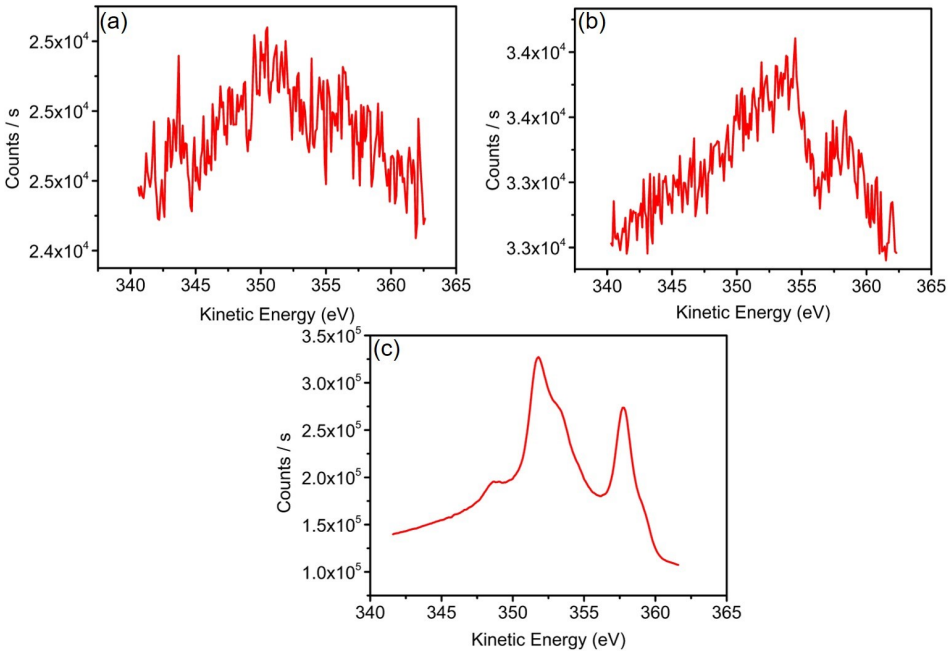

Fig. S7 Auger spectra (Ag MNN) of O-Ag@AuNCs (a), R-Ag@AuNCs (b) and metallic silver (c).

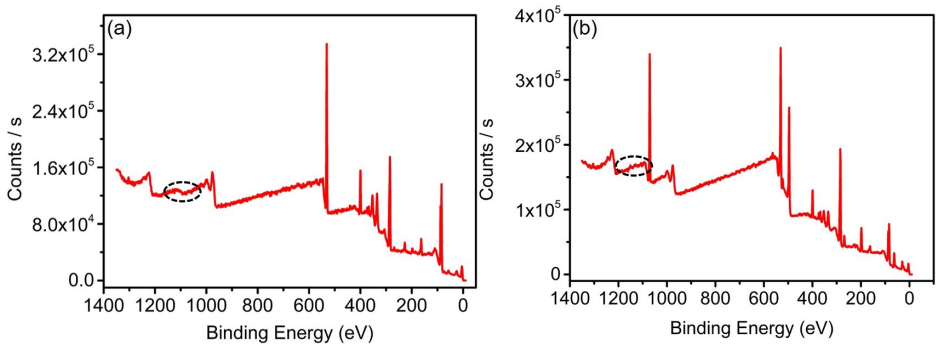

Fig. S8 XPS of O-Ag@AuNCs (a) and R-Ag@AuNCs (b). Black dotted circles represent Ag MNN area.

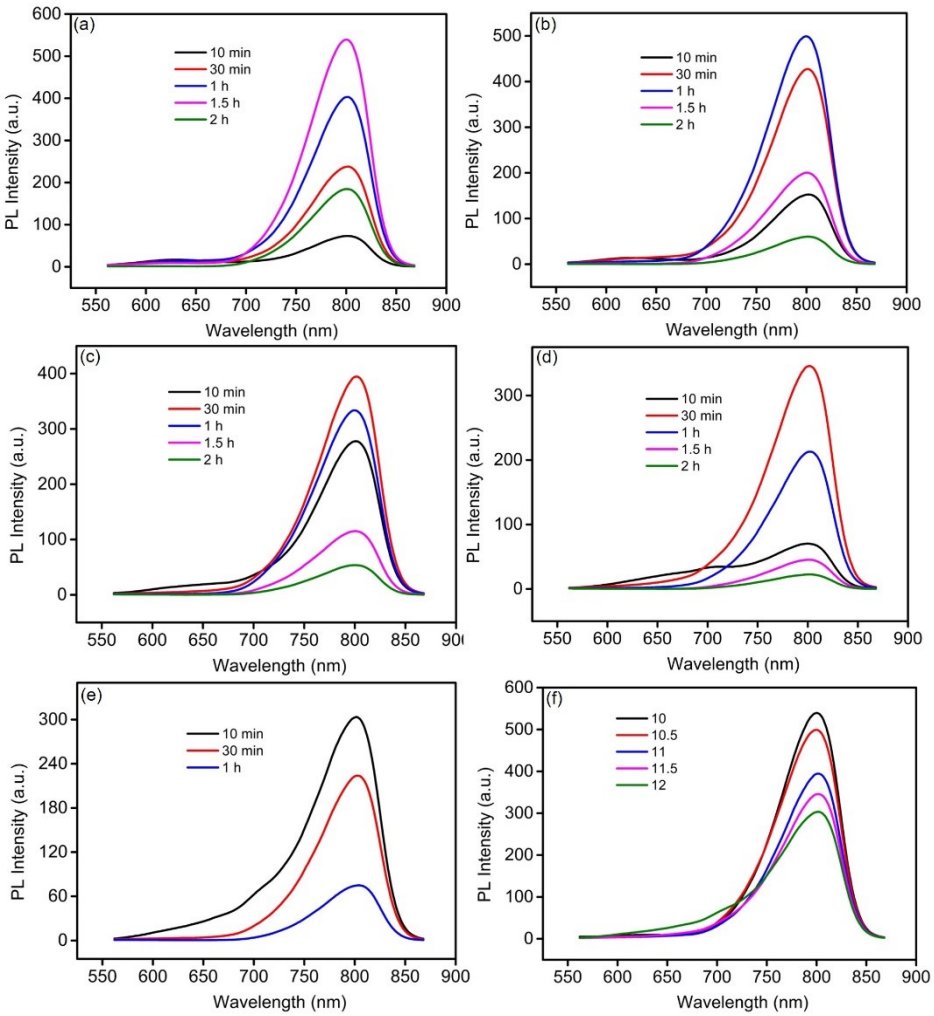

Fig. S9 (a-e) The fluorescence emission spectra of GSH-AuNCs obtained at different pH and different reaction times. (a) pH = 10; (b) pH = 10.5; (c) pH = 11; (d) pH = 11.5; (e) pH = 12; (f) Fluorescence emission spectra of GSH-AuNCs with the highest fluorescence intensity at different pH.

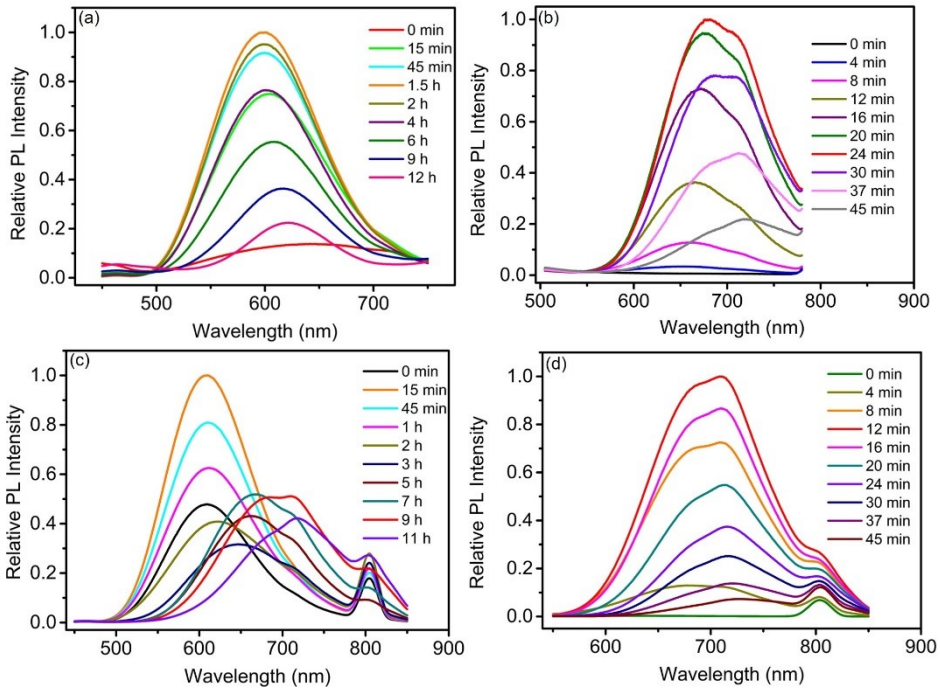

Fig. S10 The fluorescence emission spectra of O-AuNCs (a), R-AuNCs (b), O-Ag@AuNCs (c) and R-Ag@AuNCs (d) obtained at different time.

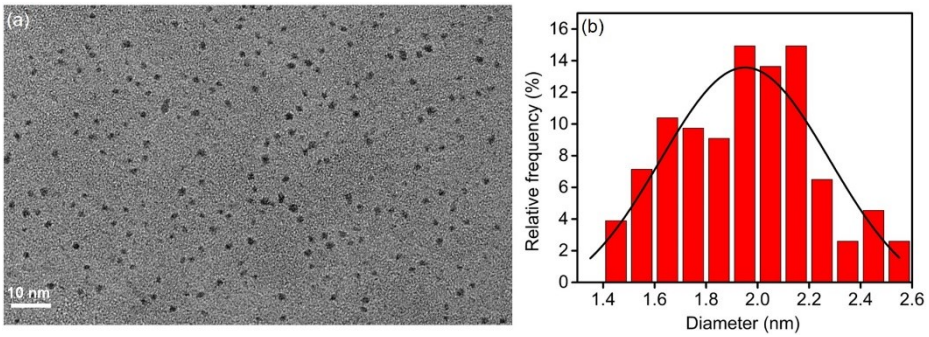

Fig. S11 (a) TEM image of the *m*R-Ag@AuNCs. (b) Size distribution of the *m*R-Ag@AuNCs. 200 particles were counted for statistical analysis.

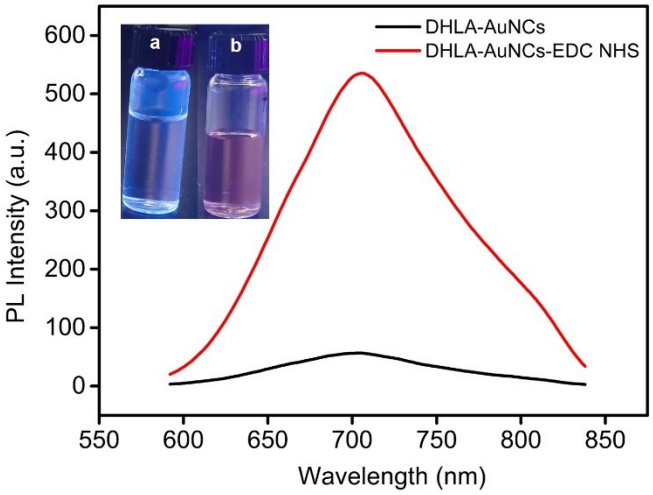

Fig. S12 Fluorescence emission spectra of the DHLA-AuNCs and DHLA-AuNCs rigidized by EDC and NHS. Insets are the photos of the DHLA-AuNCs (a) and DHLA-AuNCs + EDC + NHS (b) under a UV lamp excited at 365 nm.

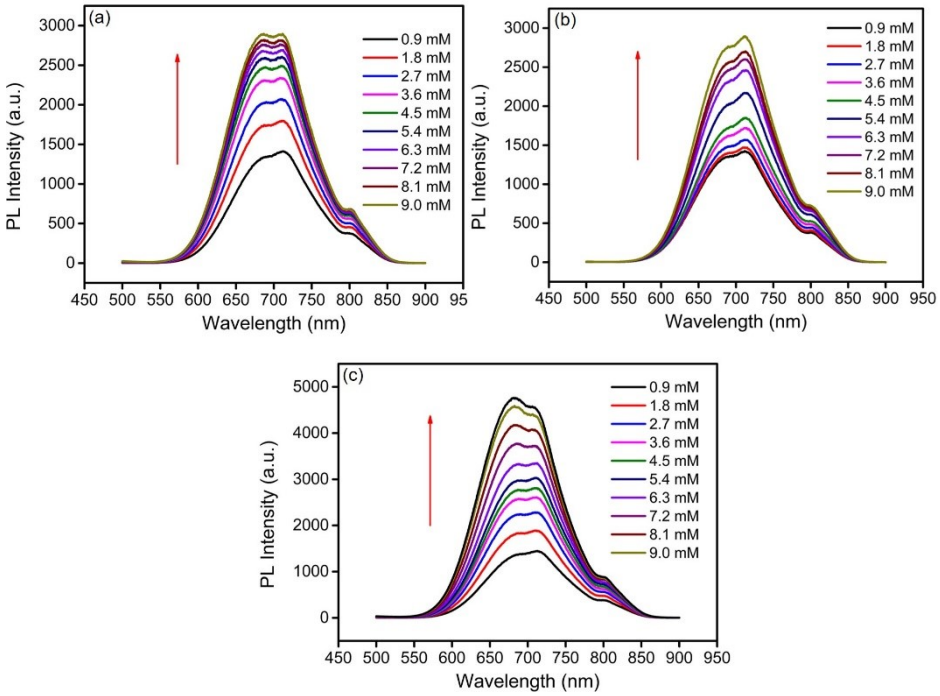

Fig. S13 Fluorescence emission spectra of R-Ag@AuNCs with EDC (a), NHS (b) and both (c).

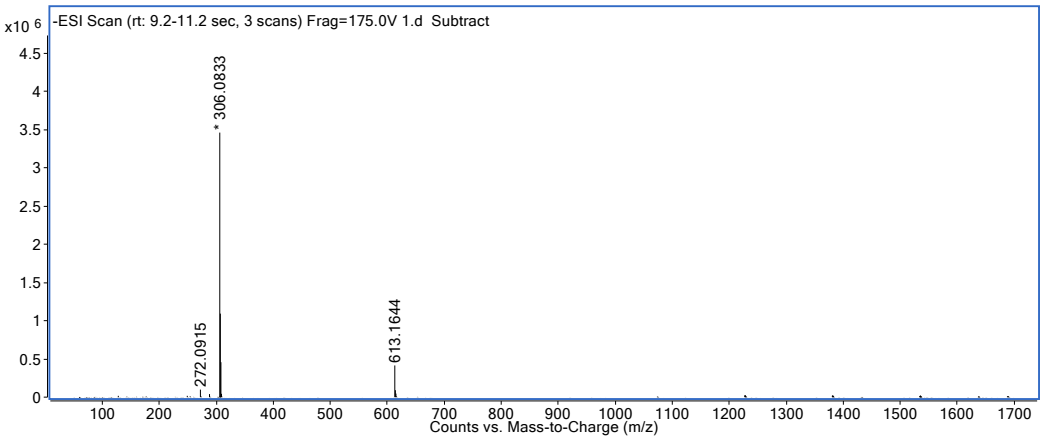

Fig. S14 ESI mass spectrum of glutathione.

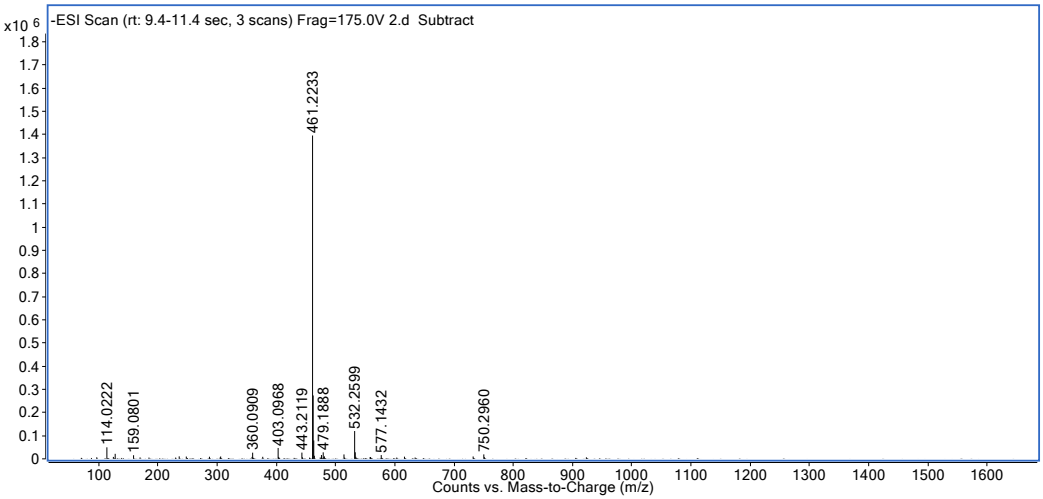

Fig. S15 ESI mass spectrum of the reaction solution of glutathione and EDC.

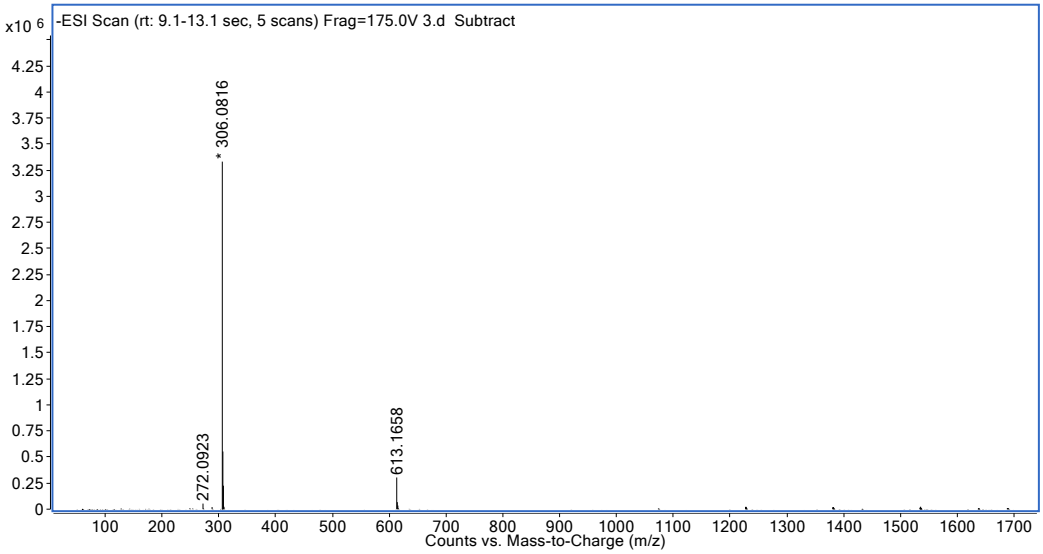

Fig. S16 ESI mass spectrum of the reaction solution of glutathione and NHS.

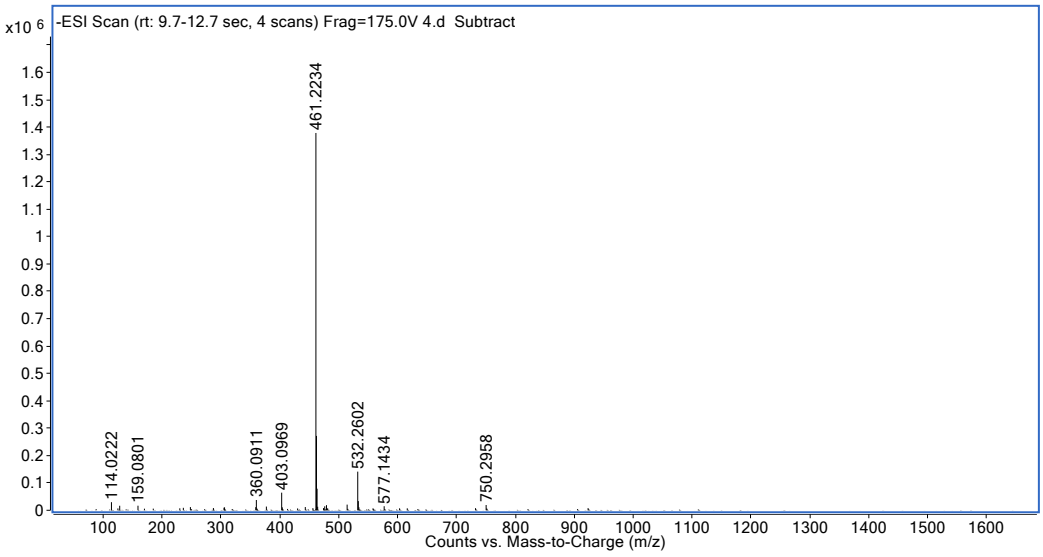

Fig. S17 ESI mass spectrum of the reaction solution of glutathione, NHS and EDC.

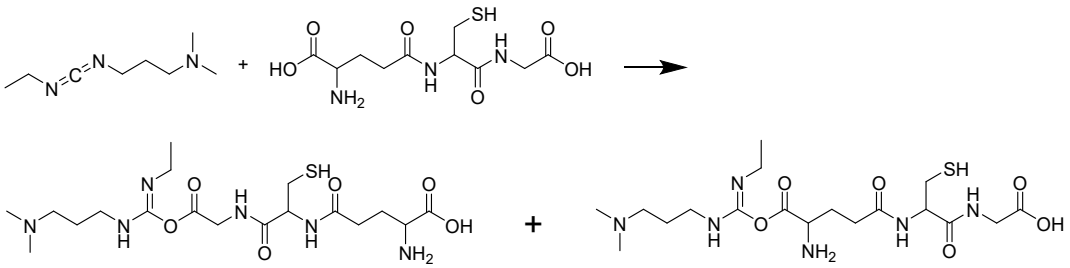

Scheme S1 The possible mechanism for the reaction of glutathione with EDC.

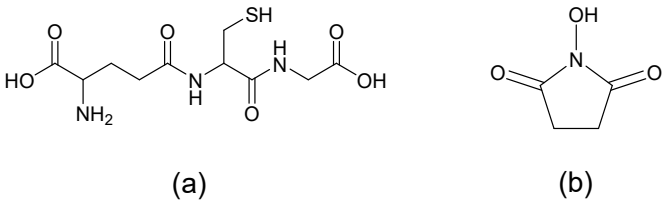

(a) (b)

Scheme S2 Molecular structure of GSH (a) and NHS (b).

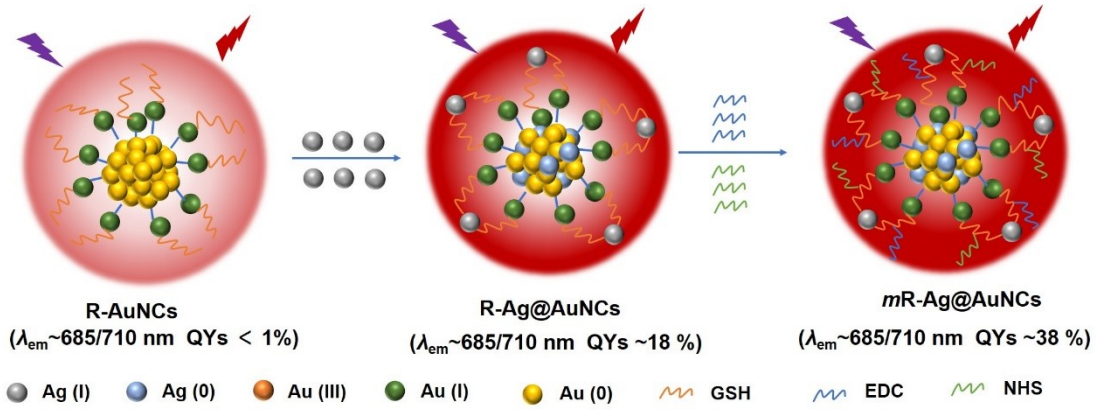

Scheme S3 The possible mechanism for the fluorescence enhancement of AuNCs.

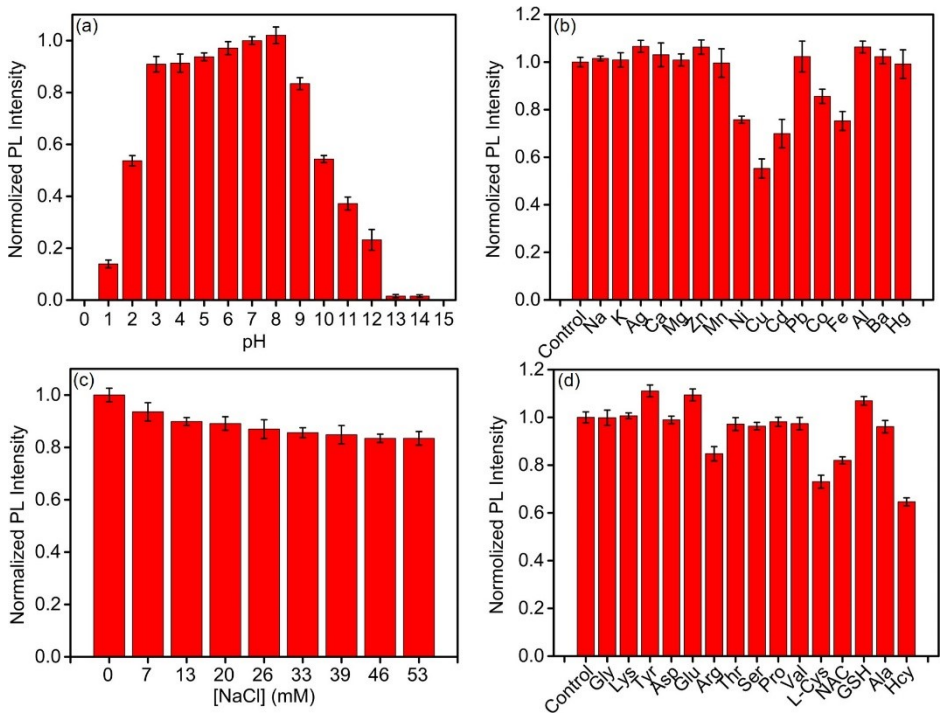

Fig. S18 Effects of pH (a), metal ions (b), NaCl (c), and amino acids (d) on the fluorescence intensity of R-Ag@AuNCs.

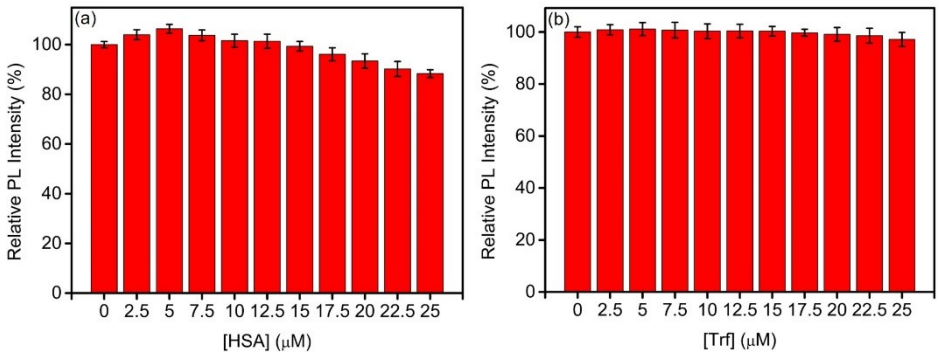

Fig. S19 Effects of human serum albumin (HSA) (a) and transferrin (Trf) (b) on the fluorescence intensity of R-Ag@AuNCs.

Fig. S20 Photos of the R-Ag@AuNCs power (a) and the *m*R-Ag@AuNCs power (b) under a UV lamp excited at 365 nm.

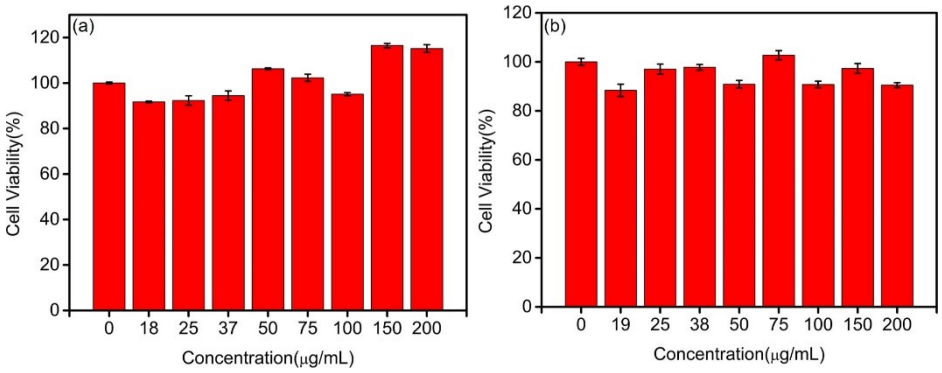

Fig. S21 Viability of HeLa cells under different concentrations of R-Ag@AuNCs (a) and *m*R-Ag@AuNCs (b).

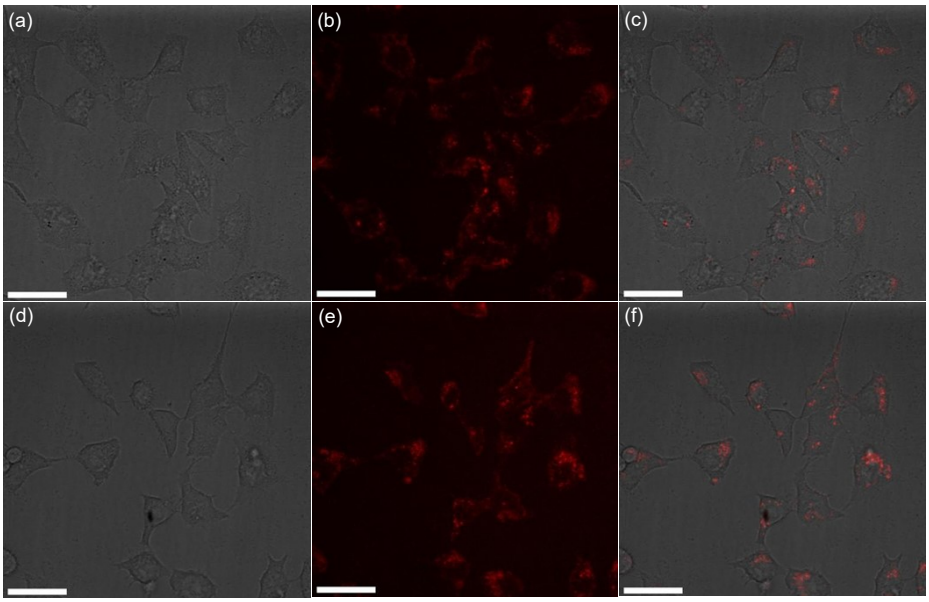

Fig. S22 Confocal images of HeLa cells incubated with 200 μg.mL^{-1} R-Ag@AuNCs (a-c) and 200 μg.mL^{-1} *m*R-Ag@AuNCs (d-f) for 4 h.

Table S2 The quantum yields of reported Au nanoclusters with red emission.

λ_m	Absolute QYs	Relative QYs	Ref
627 nm	13%	-	1
450 and 700 nm	20%	-	2
645 nm	-	4.8%	3
640 nm	26.7%	-	4
740 nm	15%	-	5
590 nm	13.5%	-	6
710 nm	38%	-	This work

REFERENCES

1 B. Yang, H. Wu and L. Zhao, *Chem. Commun.*, 2021, **57**, 5770-5773.

2 J. G. You and W. L. Tseng, *Anal. Chim. Acta*, 2019, **1078**, 101-111.

3 A. Aires, V. Fernández-Luna, J. Fernández-Cestau, R. D. Costa and A. L. Cortajarena, *Nano Lett.*, 2020, **20**, 2710-2716.

4 V. G. Deepagan, M. N. Leiske, N. L. Fletcher, D. Rudd, T. Tieu, N. Kirkwood, K. J. Thurecht, K. Kempe, N. H. Voelcker and A. Cifuentes-Rius, *Nano Lett.*, 2021, **21**, 476-484.

5 G. Pramanik, K. Kvakova, M. A. Thottappali, D. Rais, J. Pfleger, M. Greben, A. El-Zoka, S. Bals, M. Dracinsky, J. Valenta and P. Cigler, *Nanoscale*, 2021, **13**, 10462-10467.

6 Y. Li, W. Xi, I. Hussain, M. Chen and B. Tan, *Nanoscale*, 2021, **13**, 14207-14213.